The Astrophysical Journal, 712:1107–1115, 2010 April 1 doi:10.1088/0004-637X/712/2/1107

THE EFFECT OF MASS LOSS ON THE TIDAL EVOLUTION OF EXTRASOLAR PLANET

J. H. Guo[1,2]

National Astronomical Observatories/Yunnan Observatory, Chinese Academy of Sciences, P.O. Box 110, Kunming 650011, China

Received 2009 October 15; accepted 2010 February 9; published 2010 March 10

ABSTRACT

By combining mass loss and tidal evolution of close-in planets, we present a qualitative study on their tidal migrations. We incorporate mass loss in tidal evolution for planets with different masses and find that mass loss could interfere with tidal evolution. In an upper limit case ($\beta = 3$), a significant portion of mass may be evaporated in a long evolution timescale. Evidence of greater modification of the planets with an initial separation of about 0.1 AU than those with $a = 0.15$ AU can be found in this model. With the assumption of a large initial eccentricity, the planets with initial mass $\leqslant 1\,M_J$ and initial distance of about 0.1 AU could not survive. With the supposition of $\beta = 1.1$, we find that the loss process has an effect on the planets with low mass at $a \sim 0.05$ AU. In both cases, the effect of evaporation on massive planets can be neglected. Also, heating efficiency and initial eccentricity have significant influence on tidal evolution. We find that even low heating efficiency and initial eccentricity have a significant effect on tidal evolution. Our analysis shows that evaporation on planets with different initial masses can accelerate (decelerate) the tidal evolution due to the increase (decrease) in tide of the planet (star). Consequently, the effect of evaporation cannot be neglected in evolutionary calculations of close-in planets. The physical parameters of HD 209458b can be fitted by our model.

Key words: planetary systems – planets and satellites: general – stars: individual (HD 209458)

1. INTRODUCTION

There are considerable observations for exoplanets in the past several years and over 400 planets have been discovered outside of the solar system. From the side of observation it is easier to detect massive exoplanets. Jupiter-like exoplanets orbiting their host stars at a small separation of less than 0.1 AU have been detected (e.g., Table 1 of Pont 2009). To understand their interior structures and compositions, the precise masses, radii, and orbital parameters are required. An advantage of transit in finding planets is that the masses and radii of exoplanets can be determined. Thus, theoretical models can be used to constrain the interior properties of transiting exoplanets (Bodenheimer et al. 2001; Guillot & Showman 2002). The star–planet system is often considered similarly to the binary system in which tidal interaction can result in exchange between the spin angular momentum and orbit angular momentum so that their spin and orbit periods are synchronized (Zahn 1977; Hut 1980; Eggleton & Kiseleva 1998). The tidal effects on planets have been thought to explain the low e value by Rasio et al. (1996). Current researches show that close-in planets may be the consequence of tidal interaction, and the tidal action will fall off very rapidly with the separation (Jackson et al 2008, 2009). Moreover, the tidal heating has been calculated for the evolution in several studies (Gu et al. 2004; Miller et al. 2009; Ibgui & Burrows 2009). These authors found that the tidal heating is an important energy source of evolution by coupling the tidal effect to thermal evolution, but a simultaneous fit for all parameters (radius, semimajor axis, eccentricity, and age) seems to be difficult.

Vidal-Madjar et al. (2003) found evidence for atmospheric evaporation in transiting planet HD 209458b, and the estimated lower limit of the mass loss rate is 10^{10} g s^{-1}. It means that the planet could lose 10^{26} g in 10^9 yr at least. The evaporation could lead to a correlation between the mass period and surface gravity period found by Mazeh et al. (2005) and Southworth et al. (2007). The evolutionary history of the star would be considered in order to estimate a more exact mass loss rate because a higher mass loss rate is possible when the young star emits a stronger X-ray and ultraviolet (XUV) flux (Lammer et al. 2003; Penz et al. 2008). Baraffe et al. (2004, 2005) included the influence of mass loss on evolutionary calculations, and mass loss rates varying from 10^{-8} M_J yr^{-1} to 10^{-12} M_J yr^{-1} are obtained from their calculations. All the above studies showed that a significant portion of mass could be evaporated in a long evolution timescale.

In order to better understand the fundamental properties of planets, we focus on the combination between the mass loss and the tidal action. The main aim of this paper is to upgrade the tidal model with mass loss. The mass loss is coupled to the orbital evolution in this model; therefore, it can fit the semimajor axis, eccentricity, radius, and mass simultaneously. We present our models in Section 2. The results and applications are given in Section 3. In Section 4, we discuss and summarize our results.

2. THE MODEL

In this paper, we want to test the potential role of mass loss in the tidal evolution of a planet. The equations of tidal evolution on the semimajor axis and eccentricity are (Jackson et al. 2009)

$$\frac{1}{a}\frac{da}{dt} = -\left[\frac{63\sqrt{GM_s^3}R_p^5e^2}{2Q'_pM_p} + \frac{9\sqrt{G/M_s}R_s^5M_p}{2Q'_s} \times \left(1+\frac{57}{4}e^2\right)\right]a^{-13/2} \quad (1)$$

$$\frac{1}{e}\frac{de}{dt} = -\left[\frac{63\sqrt{GM_s^3}R_p^5e^2}{4Q'_pM_p} + \frac{225\sqrt{G/M_s}R_s^5M_p}{16Q'_s}\right]a^{-13/2}. \quad (2)$$

The first term in Equation (1) represents the tidal effect of the planet while the tidal effect of the star is expressed in the second

[1] Also at Department of Earth, Atmospheric, and Planetary Science, Massachusetts Institute of Technology, Cambridge, MA 01742, USA.

[2] Also at Key Laboratory for the Structure and Evolution of Celestial Objects, Chinese Academy of Sciences, Kunming 650011, China.

term. It is worth noting that the first term is proportional to $\frac{1}{M_p}$ while the second term is proportional to M_p. This implies that the mass loss in planet leads to an increase in the planetary tide, but leads to a decrease in the stellar tide. The final effect is a subtle balance between the planetary tide and stellar tide. The model assumes that the planetary orbital period is shorter than the star's rotation period. Equations (1) and (2) also show that eccentricity and semimajor axis decrease with time. In fact, Dobbs-Dixon et al. (2004) indicated that the variation of the semimajor axis depends on the ratio of the orbital angular velocity of the planet to the spin angular velocity of the parent star. The semimajor axis could increase if the orbital period of the planet is longer than the rotation period of the parent star, or vice versa. This hints that the spin angular momentum of the star can be transferred to the orbit of the planet if the rotation period of the star is shorter than the orbital period of the planet. A good example for the exchange of angular momentum is Bootis which is almost synchronized with the orbital motion of its planet (Donati et al. 2008). As a star is younger, the rotation period could be short. However, stars lose their spin angular momentum through stellar winds so that the spins of stars decline rapidly with time ($\Omega \propto t^{-1/2}$; Skumanich 1972). The orbital periods of most transiting planets are of the order of magnitude of a few days. Therefore, in most evolution times the orbital period of planet should be shorter than the stellar rotation period.

Different models have been developed to understand the process of mass loss (Yelle 2004; Lecavelier des Etangs et al. 2004; Tian et al. 2005; Erkaev et al. 2007). Lammer et al. (2003) presented that the energy deposition of X-ray and UV radiation from the parent star can lead to a high temperature, and a hydrodynamic process can occur in the planetary atmosphere. The mass loss rates of energy deposition tightly depend on the fluxes of XUV radiation. In general, young stars can radiate more energy in the XUV band than old ones. H I Lyα emission can also contribute a significant fraction for the XUV flux. Thus, the total orbit-averaged fluxes of XUV are $F_s = \frac{(F_{\rm XUV}+F_{\rm H\alpha})}{a^2(1-e^2)}$ (Barnes et al. 2008).

Based on the studies of Lammer et al. (2003) and Baraffe et al. (2004), the contributions from XUV and Lyα can be written as

$$\begin{cases} F_{\rm XUV} = 6.13 t^{-1.19} f_{\rm XUV}, & t \geqslant 0.1\,{\rm Gyr} \\ F_{\rm XUV} = F_{\rm XUV}(0.1), & t < 0.1\,{\rm Gyr} \end{cases} \quad (3)$$

$$\begin{cases} F_{\rm H\alpha} = 3.17 t^{-0.75} f_{\rm H\alpha}, & t \geqslant 0.1\,{\rm Gyr} \\ F_{\rm H\alpha} = F_{\rm H\alpha}(0.1), & t < 0.1\,{\rm Gyr}, \end{cases} \quad (4)$$

where t is the age in Gyr, $f_{\rm xuv} = 8.5 \times 10^{-4}\,{\rm W\,m^{-2}}$, and $f_{\rm H\alpha} = 1.42 \times 10^{-3}\,{\rm W\,m^{-2}}$.

For close-in planets, the tidal gravity of host star can enhance the mass loss rate (Erkaev et al. 2007). Therefore, the mass loss rates of close-in planets could be written as

$$\dot{M} = \frac{3\eta\beta^3 F_s}{G\rho K(\xi)}, \quad (5)$$

where β is the ratio of the expansion radius $R1$ to the planetary radius R_p, $R1$ is the altitude where the XUV radiation is absorbed, R_p represents the distance form the center of the planet to the 1 bar pressure level in the atmosphere, η is the heating efficiency, and ρ is the mean density of the planet. Here, $K(\xi) = 1 - \frac{3}{2\xi} + \frac{1}{2\xi^2} < 1$ is a nonlinear potential energy reduction factor due to the stellar tidal forces, and $\xi = d(\frac{4\pi\rho}{9M_*})^{1/3}$ is the Roche lobe boundary distance, where M_* is the mass of star and d is the orbital distance. Erkaev et al. (2007) assumed a circular orbit in calculating the Roche lobe enhancement factor. To account for the effect of a non-circular orbit, we replace d with the average orbital distance a in Equation (5).

The variation of radius must be considered in this model because the mass loss rate is tightly related to the mean density shown in Equation (5). The radii of planets vary due to the effects of cooling, irradiation, and tidal heating. However, the irradiation of host star does not have an evident impact on planets at a large separation. Cooling dominates the variation of planetary radius, while the irradiation of the parent star can slightly change the structure of close-in planets (Fortney et al. 2007). In general, for a given mass R_∞ decreases with the increase of separation if tidal heating is neglected (Fortney et al. 2007). However, a Jupiter-like planet only varies $\sim$0.1 $R_{\rm J}$ from 0.02 to 0.06 AU. The variation in radius of the planet at the distance larger than 0.06 AU is negligible (Burrows et al. 2007). Though the effect of evaporation could also lead to the variation in radius, we ignore the radius dependence on the evaporation in our model since only a few percent variation in the radius of Jupiter-like planet is shown in model calculations (Baraffe et al. 2004; Hansen & Barman 2007). An empirical relation for the variation of planetary radius was given by Lecavelier des Etangs (2007):

$$R_p(t) = R_\infty + \beta t^{-0.3}, \quad (6)$$

$\beta = 0.2 R_\infty\,{\rm Gyr}^{0.3}$ for $M_p \gtrsim 0.3\,M_{\rm J}$, and with $\beta = 0.3 R_\infty\,{\rm Gyr}^{0.3}$ for $M_p \approx 0.1\,M_{\rm J}$. The relation shows that the radius of planet is not sensitive to its mass shown by the relation. Recently, Miller et al. (2009) and Ibgui & Burrows (2009) found that the radius could increase with time because of the tidal heating when they incorporated the tidal heating into an evolutionary code. The simple scaling law (Equation (6)) should be revised with consideration of tidal heating. However, in this paper we focus on the generic character of the combination between the mass loss and the orbital evolution more than on the final effect of incorporating them into evolutionary models. Hence, the scaling law of radius is applied in all of our models.

3. RESULTS

We can integrate Equations (1) and (2) from 10^7 yr (disk depletion timescale) to 15×10^9 yr (cosmic age) by using Equations (3)–(6). The integration is terminated in two cases as follows: (1) the mass of planet is lower than 0.01 $M_{\rm J}$ because the evolution of planet is similar to that of Earth-like planet in the range of mass; (2) the pericenter distance is smaller than the solar radius, 0.005 AU. We assume that all planets originate at a large semimajor axis according to the decreases in the separation with time shown by Equation (1). The initial mass, eccentricity, semimajor axis, and radius R_∞ must be set in this model. For the sake of comparison, we set the values of the initial mass at 0.7 $M_{\rm J}$, 1.0 $M_{\rm J}$, 2.0 $M_{\rm J}$, and 5.0 $M_{\rm J}$, the orbital separation at 0.05 AU, 0.1 AU, and 0.15 AU, and the initial e at 0.7. R_∞ is constrained from evolutionary models and observed measurements. From the theoretical side, the radius evolves with time toward a constant and R_∞ for the coreless planets is about 1.1 $R_{\rm J}$ (Baraffe et al. 2004; Burrows et al. 2007; Fortney et al. 2007), while in observation the observed radius varies mainly from 0.975 to 1.3 $R_{\rm J}$ (http://exoplanet.eu). So, $R_\infty = 1.1\,R_{\rm J}$

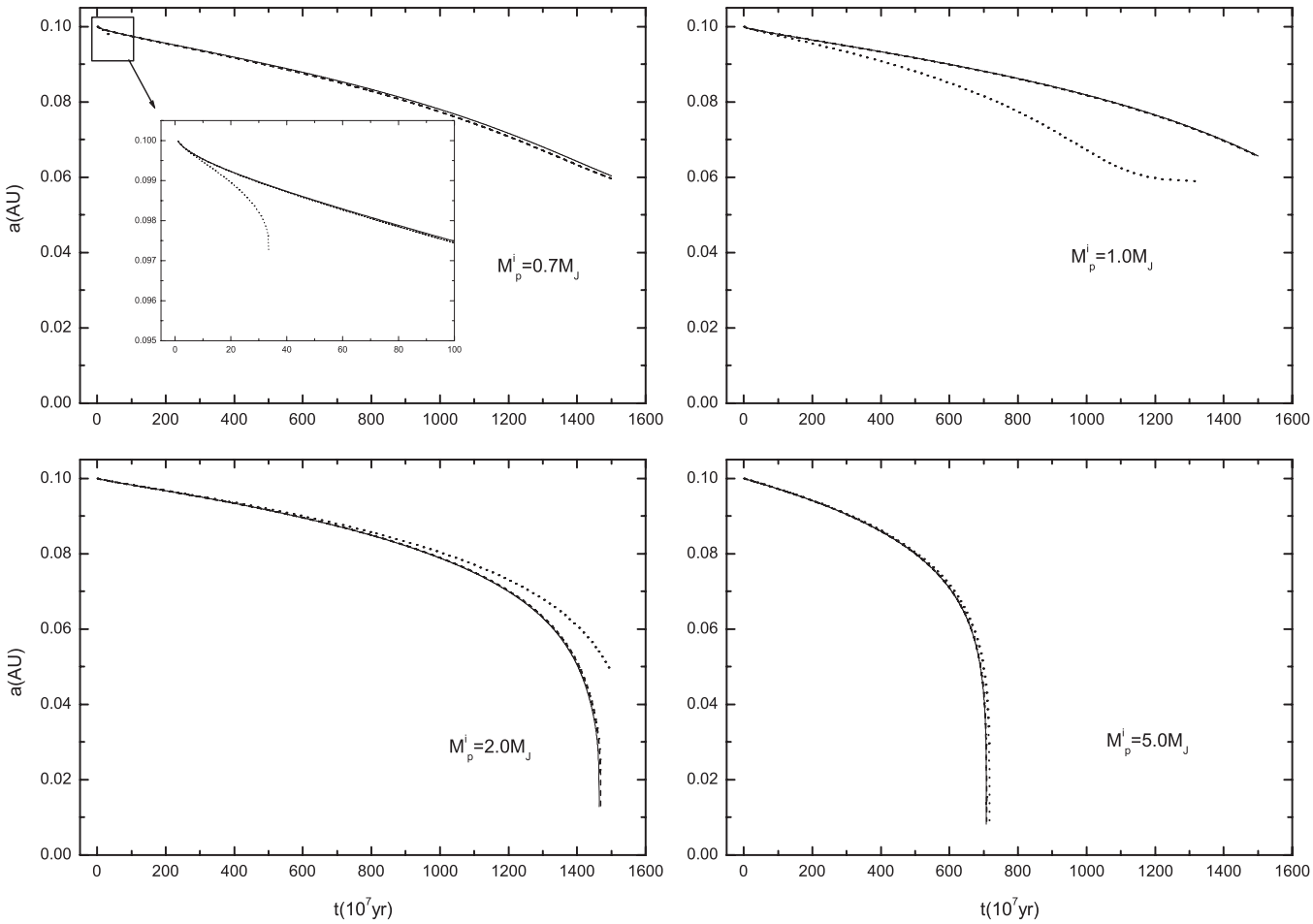

Figure 1. Evolutions of orbit with different masses $M_i = 0.7$, 1.0, 2.0, and 5.0 M_J. The initial a and e are 0.1 AU and 0.7, respectively. The solid lines represent the non-evaporating models. The dashed and dotted lines correspond to evaporating models with $\beta = 1.1$ and 3.

becomes our final choice. The model also depends on the tidal dissipation parameters Q_s and Q_p. Jackson et al. (2008) found that the best fits of stellar and planetary Q are $\sim 10^{6.5}$ and $\sim 10^{5.5}$, respectively. We adopt Jackson's results in our model.

Based on the hydrodynamic model of Watson et al. (1981), Lammer et al. (2003) estimated $\beta = 3$, but it could be unity according to recent hydrodynamic models which showed that the expansion radius could be 1–1.5 R_p (Yelle 2004; Murray-Clay et al. 2009). Lammer et al. (2009) also thought the mass loss rate was overestimated with $\beta = 3$ by Baraffe et al. (2004). Since the model of Lammer et al. (2003) yields maximum energy limited escape, it is important to examine its consequences on the fate of the planet. We discuss both cases: one is $\beta = 3$ as upper limit and the other is $\beta = 1.1$ in hydrodynamic models (Murray-Clay et al. 2009). In our models, the stellar mass and radius are set as 1 $M_\odot$ and 1 $R_\odot$, respectively.

3.1. Tidal Evolution with Maximum Escape Rate ($\eta = 100\%$)

3.1.1. Models with $\beta = 3$

With the full energy-limited condition, the heating efficiency $\eta = 100\%$. Figures 1–3 show the evolutions of planets with different masses at 0.1 AU. For comparison, we present the models without mass loss as a solid line in Figures 1–3. As shown in the top left panel of Figure 1, the behaviors of models with $\beta = 3$ (**beta3**, dotted line) are different obviously from those of models with $\beta = 1.1$ (**beta1.1**, dashed line) in the case of 0.7 M_J. As shown in Figure 3, the mass in the **beta3** model decreases rapidly with a mass loss rate in the order of magnitude of 10^{-9} M_J yr^{-1} at the very beginning of evolution, and it is lost entirely within 0.4 Gyr. For a low mass planet, the tidal evolution is sensitive to the change in mass because it is dominated by the planetary tide which, shown as the first term in Equation (1), is larger than the stellar tide, shown as the second term. Consequently, the decrease in the mass of a low mass planet speeds up the decay of its orbit. Moreover, the closer the orbit, the slower the mass loss rate decreases due to more the deposit energy increases in unit area. It seems a runaway process in which planet loses entire mass in an intermediate age.

The effect of mass loss is significant in the case of **beta3** for $M = 1.0\,M_J$ (the top right panel of Figure 1). The track of the model with mass loss shows an obvious difference with that of the model with a constant mass, and its mass is lost entirely within 14 Gyr. In the 1.0 M_J model, the increase in planetary tide can be compensated in part by the decrease in stellar tide because the effect of the planetary tide is slightly greater than that of the stellar tide. But for a high mass planet, the orbital evolution is dominated by the stellar tide which is proportional to the planetary mass. Thus, the lower the mass, the slower the evolutions of eccentricity and semimajor axis are. In other words, only 12% of mass in the model of 2.0 M_J and only 2% of mass in the model of 5.0 M_J are lost within 15 Gyr (Figure 3). So, the mass loss is not important for the evolution of a high mass planet any more. It is worth noting that the model with 5.0 M_J spirals into its parent star in about 7 Gyr, and both the model with evaporation and the model without evaporation

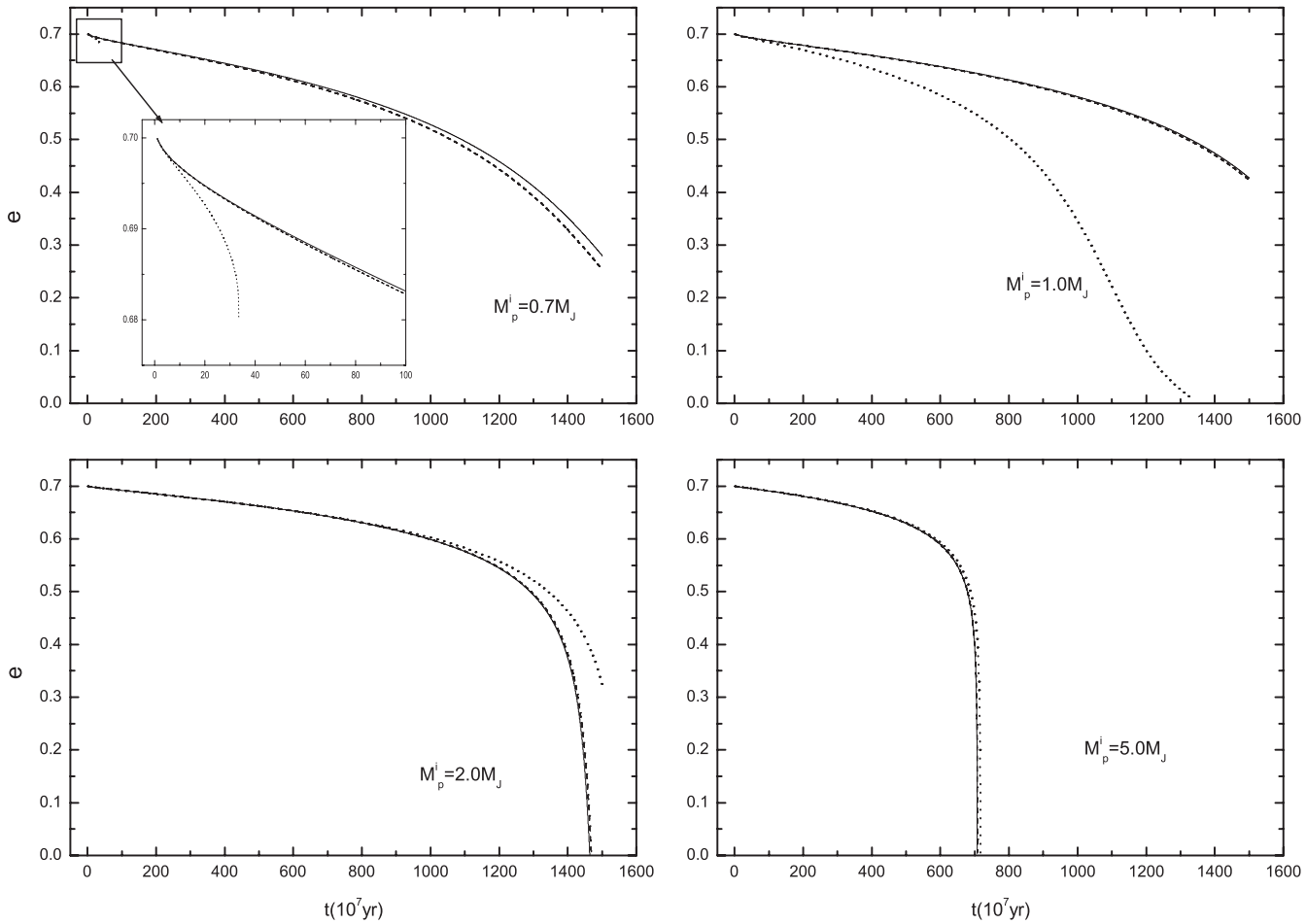

Figure 2. Evolutions of e with different masses (M_i = 0.7, 1.0, 2.0, and 5.0 M_J) when the initial e is 0.7 and the initial a is 0.1 AU.

have the same effect on the evolution. Two reasons led to this consequence: (1) the increase in the stellar tide caused by the high mass of planet makes the tidal evolution very rapid and (2) the mass loss rate of the massive planet is smaller than that of the light planet in that the density of the massive planet is higher than that of the light planet with the assumption of the same radius for all planets.

In all the models, the evolution of eccentricity closely follows that of the semimajor axis (Figure 2). It is reasonable that all models have similar behaviors induced by the same physical causes for the change of eccentricity. The lower limit of e in 0.7 M_J planets is $e \sim 0.68$ (the top panel of Figure 2), while the values of e can reach zero in the models with 1 and 5 M_J. The circularizing timescale is also affected by the variation of the semimajor axis. Consequently, it is possible that the circularizing timescale is longer than the planet lifetime with certain initial values of e and a.

With the decrease in the initial semimajor axis, different behaviors occurred in the evolutionary trajectories. With the initial value of $a = 0.05$ AU, we also plot a and e as a function of time for all the models in Figures 4 and 5, respectively. The models with $a = 0.05$ AU show shorter lifetime due to stronger tidal action, and the tidal effect is still important up till $M_p = 2.0\,M_J$. In the models with the initial mass of 0.7 M_J and with the initial mass of 1.0 M_J, the entire mass is exhausted in the runaway process caused by mass loss from 0.03 Gyr to 0.05 Gyr. The result is not unreasonable because a relatively high mass loss rate caused by the very strong fluxes of XUV from the host star in the very early time can make the decay

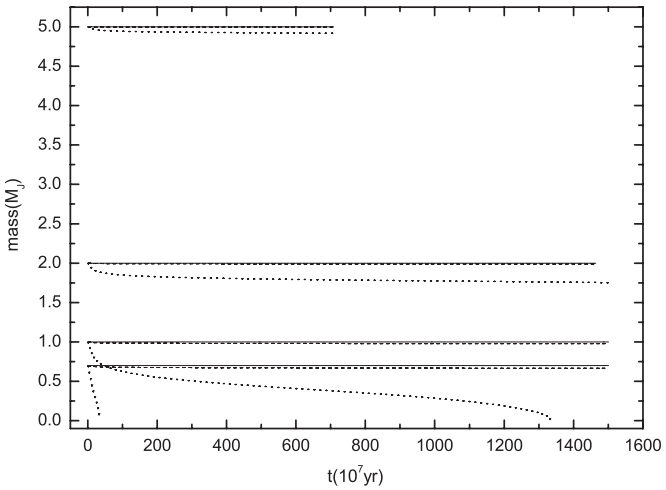

Figure 3. Evolutions of mass with different values (M_i = 0.7, 1.0, 2.0, and 5.0 M_J) when the initial $a = 0.1$ AU and the initial $e = 0.7$.

of orbit very rapid. The mass loss rate remains nearly constant because the decrease in density rendered by the lost significant portion of the mass can counteract the decline of F_{XUV}. As the planet approaches its host star, the flux in unit area even becomes larger. Therefore, the high mass loss rate even makes the planet exhausted in a short timescale (Figure 6). For non-evaporating models, the planets can exist for a longer time than evaporating models, but all planets spiral into their host stars within 0.2 Gyr. An example of the short-life planet is WASP-18b. Hellier et al.

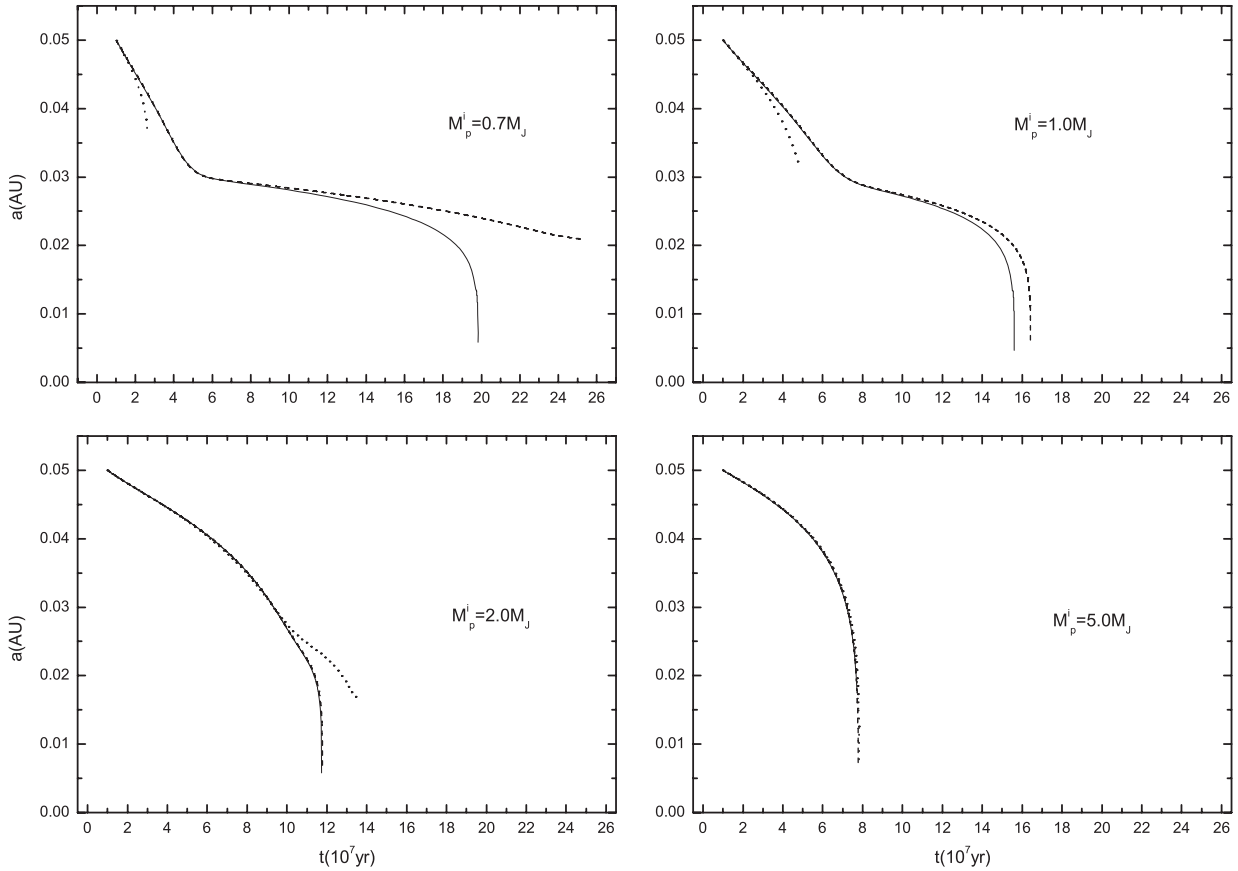

Figure 4. Evolutions of orbit with different masses $M_i = 0.7$, 1.0, 2.0, and 5.0 M_J when the initial $a = 0.05$ AU and the initial $e = 0.7$.

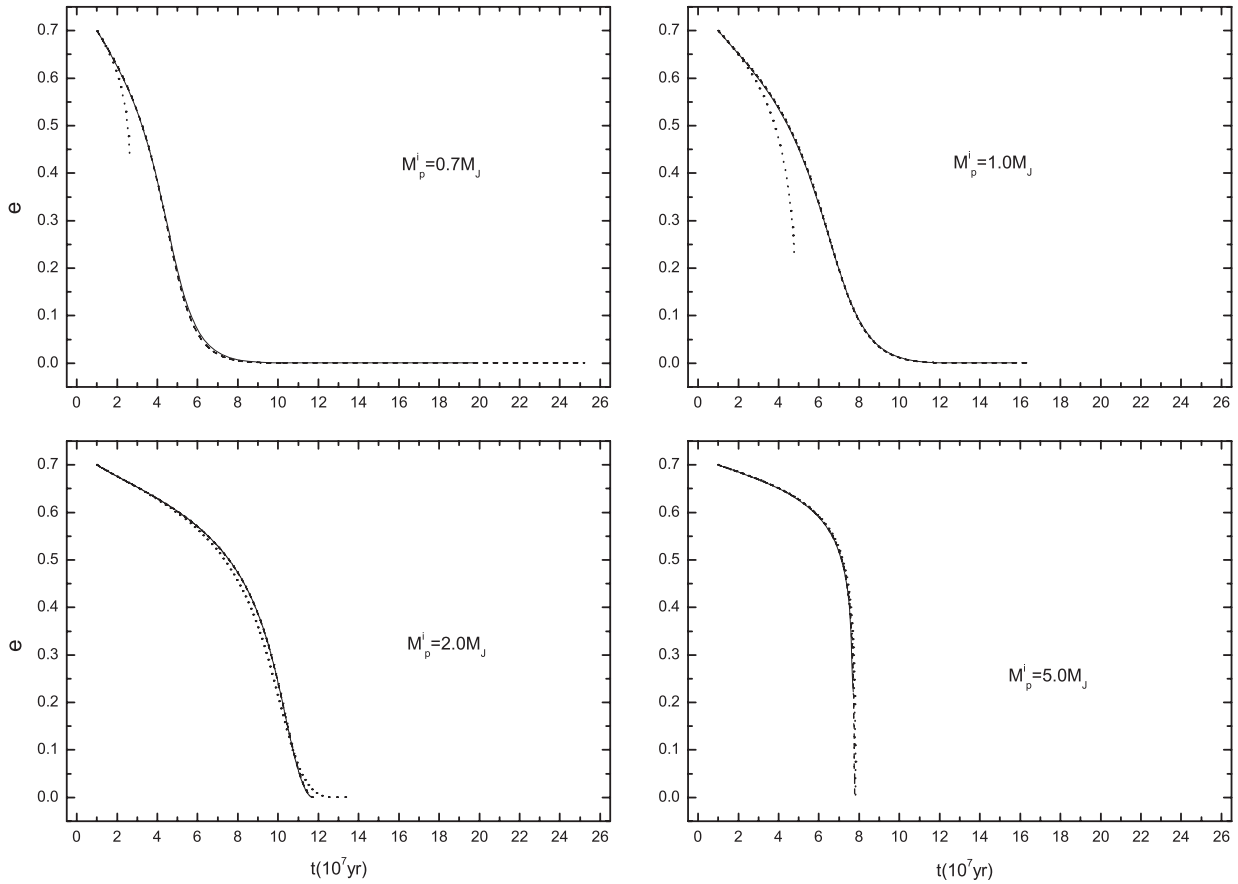

Figure 5. Evolutions of e with different masses ($M_i = 0.7$, 1.0, 2.0, and 5.0 M_J) when the initial e is 0.7 and the initial a is 0.05 AU.

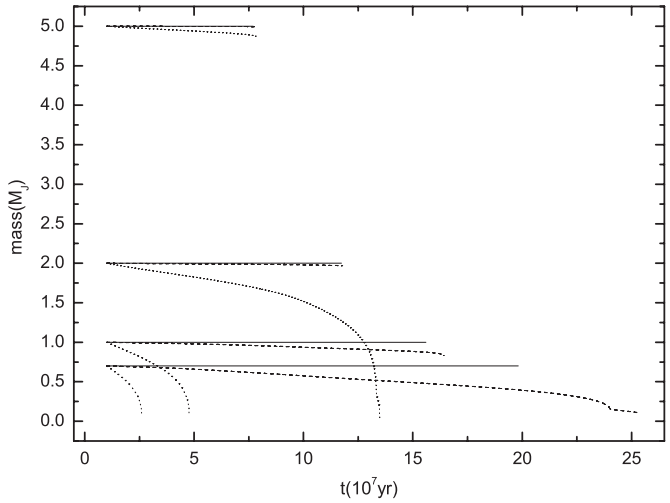

Figure 6. Evolutions of mass with different masses (M_i = 0.7, 1.0, 2.0, and 5.0 M_J) when the initial a = 0.05 AU and the initial e = 0.7.

(2009) suggested that the life of WASP-18b is very short with the assumption of $Q_s = 10^6$.

The top panels in Figure 5 show that the values of e reach zero in the non-evaporating models with the masses of 0.7 M_J and 1.0 M_J before planets collapse into their host stars. Note that the circularization timescale is shorter than the decay timescale of the semimajor axis in the case of no mass loss. For massive planets, the whole evolution of the values of e in the models with evaporation is nearly same as that in the models without evaporation. Both e and a reach zero simultaneously.

As can be see from the above discussion on separation, the effect of tide is closely related to the distance. Thus, we also test the models in the case of a = 0.15 AU. Comparing with the cases of short distance, the effect of tide can be neglected in the case of 0.15 AU. Only a few percent of variations in eccentricity and semimajor axis can be seen (Figures 7 and 8). The planets with the masses of 0.7 M_J and 1.0 M_J lose a significant portion of mass during 15 Gyr (Figure 9), while only a minor portion of mass is evaporated from massive planets.

3.1.2. Models with β = 1.1

No significant influence of mass loss is found in the **beta1.1** model at a = 0.1 AU and a = 0.15 AU (see the dashed lines in Figures 1–3 and 6–9. Note that the dashed lines can be hardly distinguished from the solid lines.). It is not unreasonable because the mass loss rate in the **beta1.1** model decreases 60 fold compared with the **beta3** model. The dashed line in Figures 3 and 9 shows that for the planets with low mass only 1%–3% of the masses are lost in 15 Gyr.

However, our study indicates that the mass loss has an evident influence on tidal evolution with the decrease in the initial semimajor axis (a = 0.05 AU). Figures 4–6 clearly show the variations in semimajor axis, eccentricity, and mass of the close-in exoplanets with low mass. Thermal evaporation could be an efficient loss process when exoplanets are close to their host stars, and the effect of Roche lobe is also remarkable due to $\xi \propto d$. Gas giants with low mass (0.7 M_J) even lost entire mass within 0.25 Gyr. Gas giant with a mass of 1 M_J lost about 20% of its mass. We also note that the evolution of eccentricity is not

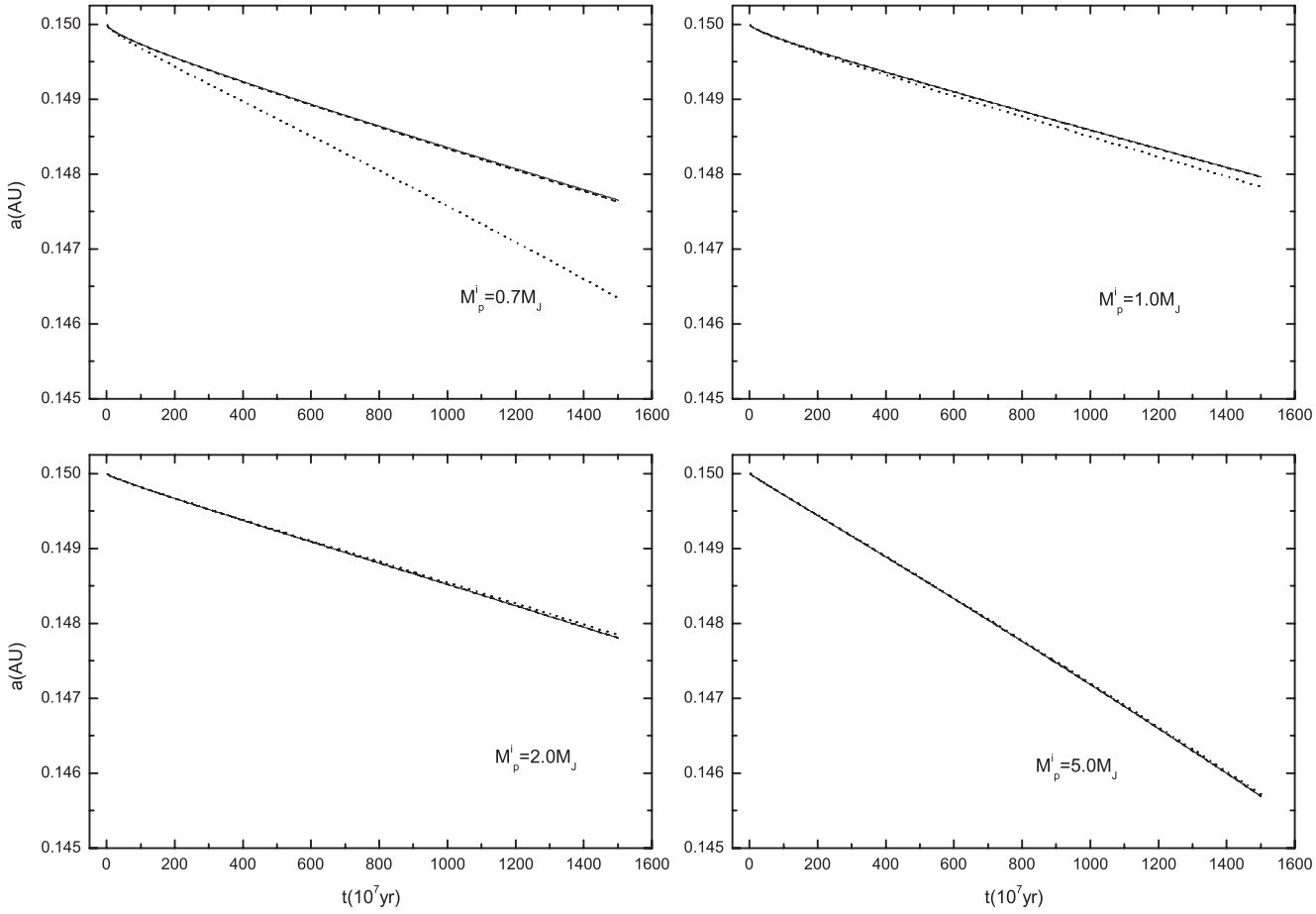

Figure 7. Evolutions of orbit with different masses M_i = 0.7, 1.0, 2.0, and 5.0 M_J when the initial a = 0.15 AU and the initial e = 0.7.

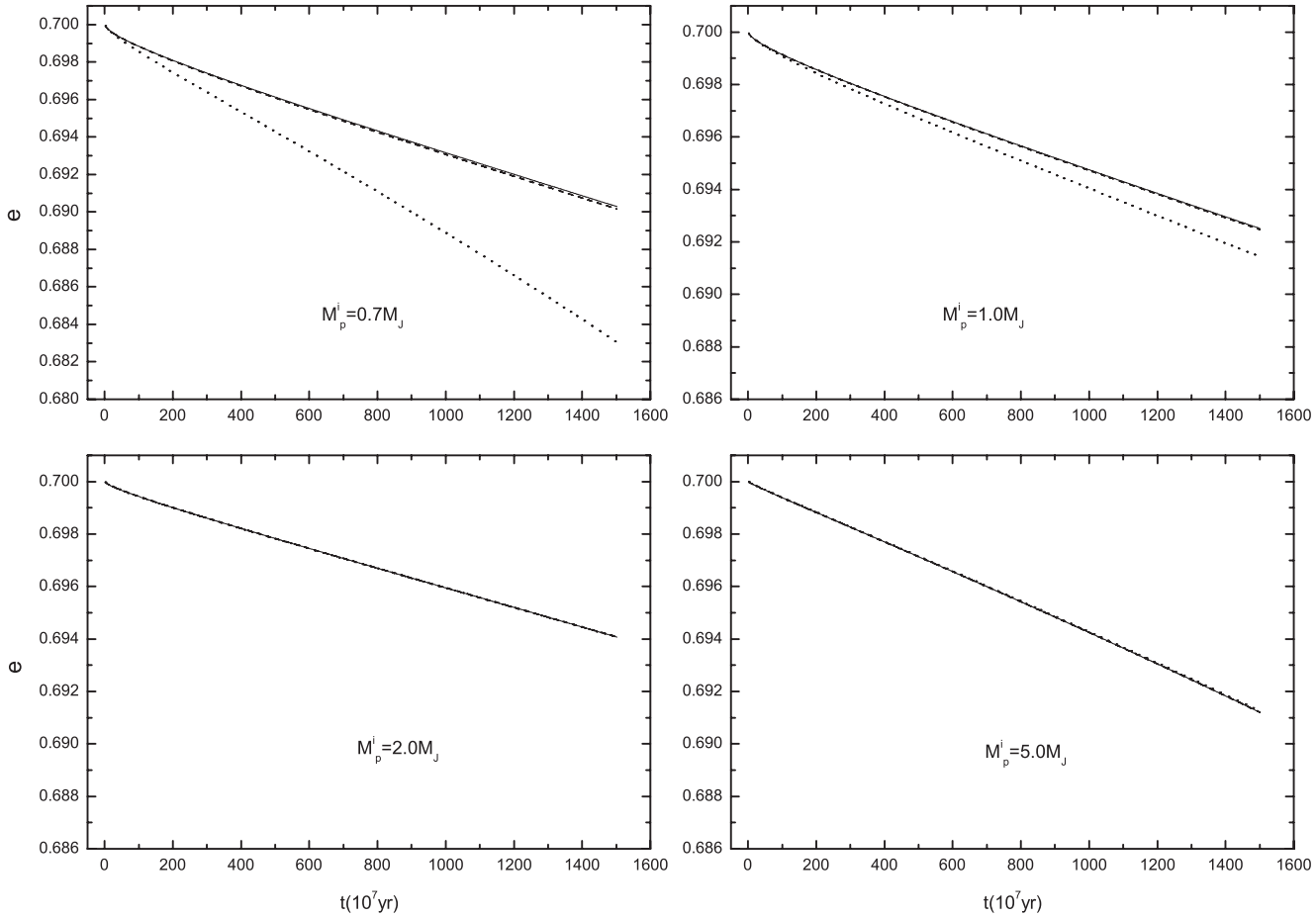

Figure 8. Evolutions of e with different masses (M_i = 0.7, 1.0, 2.0, and 5.0 M_J) when the initial e is 0.7 and the initial a is 0.15 AU.

affected by the loss process due to short circularizing timescale. As discussed in Section 3.1.1, the evolution of giant planets with greater mass, which is dominated mainly by their host stars, and thus mass loss, has no significant influence on them.

3.2. Heating Efficiency

The principal aim of the present theoretical investigation is to understand the influence of mass loss on the tidal migration, including how the heating efficiency affects the evolutionary tracks. In fact, heating efficiency varies with planetary radius. In general, the heating efficiency is higher due to the higher density at the base of the flow (Yelle 2004). An actual heating efficiency is unable to be calculated until the hydrodynamic equations are solved. Therefore, we apply a fixed heating efficiency to the entire flow. With three different heating efficiencies of 25%, 50%, and 100%, the evolutionary tracks of the planet with an initial mass of 0.7 M_J are shown in Figure 10. As shown in Figure 10, the evolutions of the semimajor axis are indeed controlled by heating efficiency. The lower the heating efficiency is, the smaller the influence of mass loss. But, even the heating efficiency of 25% can result in a significant variation in the evolution of exoplanets with low mass. Therefore, we can draw the conclusion that the loss process has obvious influence on the tidal evolutions of close-in gas giants with low mass.

3.3. Initial Eccentricity

Since the tidal model closely depends on the initial eccentricity (Equations (1) and (2)), a quantitative test for models with different initial eccentricities (e^i) is necessary. As mentioned above in Section 3.1, the mass loss leads to a small variation on massive planets. Thus, we only test planets with low mass in this section.

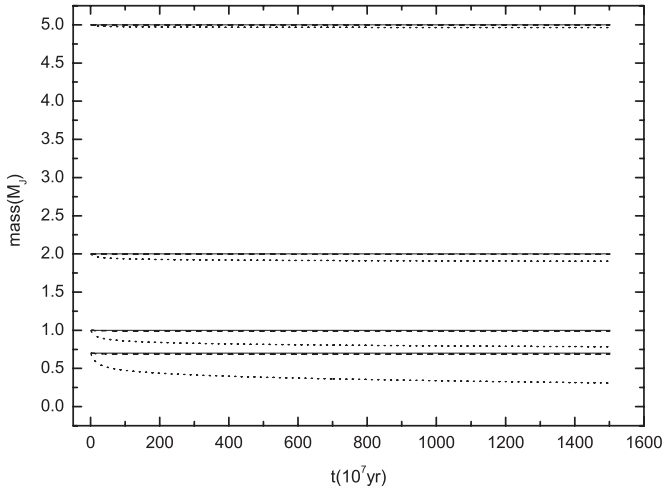

Figure 9. Evolutions of mass with different masses (M_i = 0.7, 1.0, 2.0, and 5.0 M_J) when the initial a = 0.15 AU and the initial e = 0.7.

With the assumption of full energy limited condition, we calculate models with different values of e^i under the conditions of $M^i = 0.7\,M_J$ and $a^i = 0.05$ AU. Figure 11 shows the evolutionary tracks of the semimajor axis a and mass with different values of e^i. The difference between the evaporating models and the non-evaporating models is enlarged with the decrease in e, and the smaller the value of e^i is, the longer the

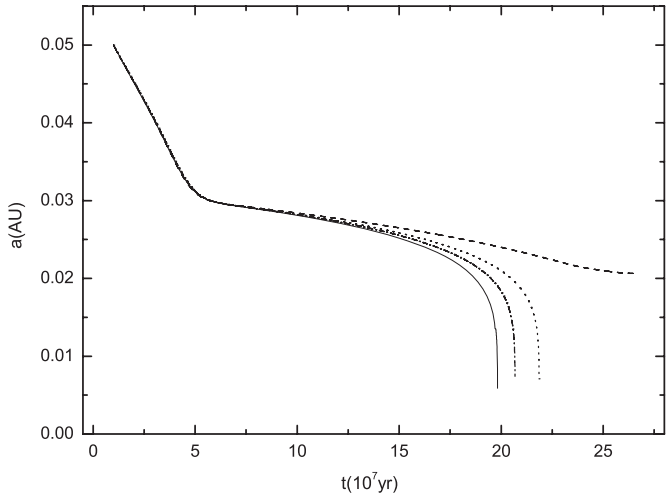

Figure 10. Evolutions of evaporating planet with three different heating efficiencies: 100% (dashed), 50% (dotted), and 25% (dash-dotted) when $M_i = 0.7\,M_J$ and $a = 0.05$ AU. The solid line represents the non-evaporating model.

evolutionary times becomes (order from left to right: $e^i = 0.7$, 0.5, 0.3, and 0.1 in Figure 11). The significant reductions in the initial eccentricity make the tidal evolution slower. Hence, those planets originated at the low value of e^i could plunge into their host stars before all of the mass are lost entirely.

3.4. Application

In this section, we apply our model to a particular sample of planet. A typical planet is HD 209458b with the radius of 1.32 R_J, the mass of 0.685 M_J, and the semimajor axis of 0.047. The observed upper limit on the orbital eccentricity is 0.028 (Ibgui & Burrows 2009). Observational data of HD 209458 are summarized in Table 1. We calculate a grid covering a large range with 16 initial masses from 0.7 M_J to 1.5 M_J ($0.7\,M_J < M_p < 1.5\,M_J$, 0.05 M_J as a step), 32 initial eccentricities from 0 to 0.8 ($0 \leqslant e \leqslant 0.8$, 0.025 as a step), and 40 initial semimajor axes from 0.05 AU to 0.15 AU (0.05 AU $\leqslant a \leqslant$ 0.15 AU, 0.025 AU as a step), as well as we test the effect of R_∞ from 1 to 1.2 R_J (0.005 R_J as a step).

A limit on the age of HD 209458b must be estimated in order that its properties are matched better. Melo et al. (2006) estimated that the age of HD 209458b is greater than 2 Gyr. Here, we assume the age to be 4 Gyr (Arras & Bildsten 2006). The mass loss is calculated within a period of 4 Gyr with four different values of heating efficiency (25%, 50%, 75%, and 100%) and with $\beta = 1.1$. In contrast with observations, the best fits for HD 209458b with four different values of heating efficiency are selected and summarized in Table 2.

Table 1
Observation Data of HD 209458b

Planet	a (AU)	e	M_p (M_J)	R_p (R_J)
HD 209458b	$0.047^{+0.00046}_{-0.00047}$	< 0.028	$0.685^{+0.015}_{-0.014}$	$1.32^{+0.024}_{-0.025}$

Note. Data are from Ibgui & Burrows (2009).

Table 2
The Best Fits for HD 209458b

η	$M_{\rm model}(M^i)$	$R_{\rm model}(R^i_\infty)$	$a_{\rm model}(a^i)$	$e_{\rm model}(e^i)$
25%	0.678(0.70)	1.319(1.165)	0.0469(0.060)	0.001(0.200)
50%	0.671(0.70)	1.324(1.170)	0.0467(0.083)	0.027(0.625)
75%	0.688(0.75)	1.324(1.170)	0.0473(0.063)	0.002(0.275)
100%	0.691(0.75)	1.319(1.165)	0.0475(0.078)	0.02(0.550)

Notes. The best-fit parameters are marked with the subscript model. The initial parameters marked with the superscript i are written within brackets. The unit of mass is in M_J, radius in R_J, and a is in AU.

The best-fit model in the case of $\eta = 25\%$ is that with $M_p = 0.678\,M_J$, $a = 0.0469$ AU, $e = 0.001$, and $R = 1.319\,R_J$, and only 3.2% of the initial mass is lost during 4 Gyr. If the full energy limited condition is considered into the model, the mass loss would be 7%. It is difficult to determine the actual heating efficiency from our model. As shown in Table 2, all the models can reproduce the observation results. Because the evolutionary history of a planet is changed with the heating efficiency, more constraint conditions should be used to determine the heating efficiency. In addition, the initial eccentricity (e^i) in all the models of Table 2 is low or in the middle, while the higher e^i is calculated with the assumption of constant mass by Ibgui & Burrows (2009).

The important problem for HD 209458b is which physical mechanism causes such as large radius. On the one hand, the enhancement of atmospheric opacity can make the radius of

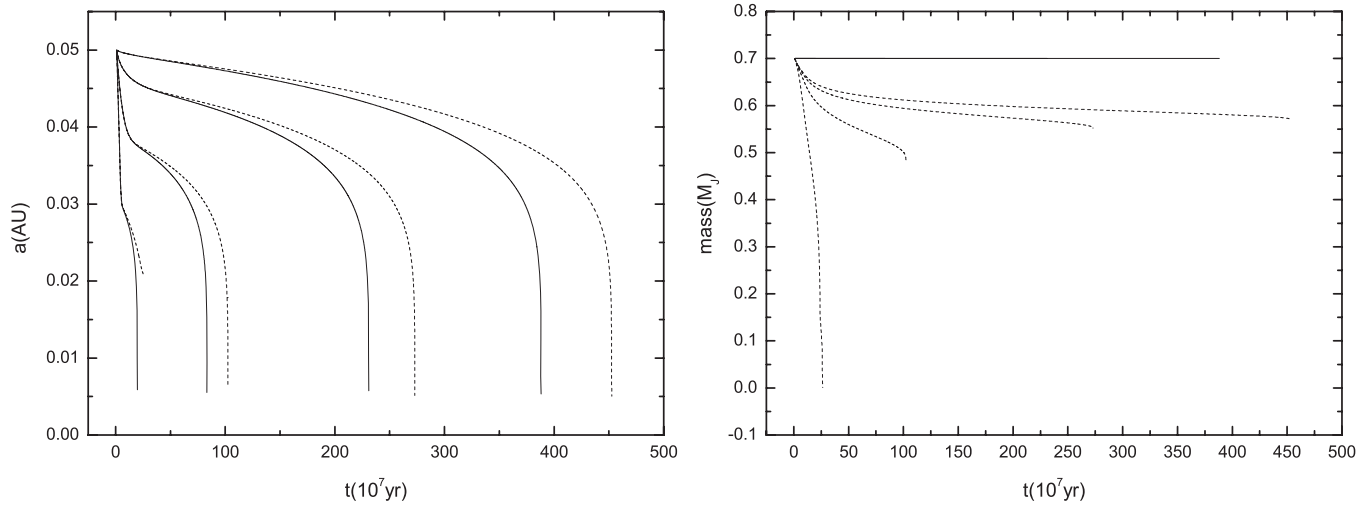

Figure 11. Left panel: evolutions of the semimajor axis with different e (from left to right: $e = 0.7$, 0.5, 0.3, and 0.1) when $M_i = 0.7\,M_J$ and $a = 0.05$ AU. Right panel: evolutions of mass with different e (from bottom to top: $e = 0.7$, 0.5, 0.3, and 0.1). Solid lines: non-evaporating models. Dashed lines: evaporating models.

HD 209458b extend to the observed radius. On the other hand, the tidal heating can also lead to the same consequence. As shown by Ibgui & Burrows (2009), the tidal heating is extremely sensitive to the value of e. The small and middle values of e^i imply the low tidal heating rate but a longer heating time. Our results suggest a small a and a low (middle) e^i which lead to a slow decrease in separation and a longer heating time during 4 Gyr. In the case of a higher e, both e and a decrease drastically so that the planet could collapse into its host star before it arrives at the current observation location.

4. DISCUSSIONS AND CONCLUSIONS

One of the possibilities for close-in planets to survive at short separation is that the planets have the solid cores. If the density of the core equals the density of Earth ($\sim$5 g cm^{-3}), the radius of the core can be estimated with its mass. For a core with a mass of 20 $M_\oplus$, its radius is 10^9 cm. Whether or not the core has a gas envelope is important to determine the radius of the core because a small gas mass can contribute a large factor to the radius of the planet (Seager et al. 2007). Adams et al. (2008) found the increase in the radius of a planet because of a gas envelope. Their results showed that the core radius of the planet with a mass of 20 $M_\oplus$ could be expanded 50% if the mass of a gas envelope equals the Earth mass. To examine whether the solid core can survive, the detailed models for planets should be calculated. The envelopes of the very close-in planets with solid cores could be stripped off due to strong XUV radiation from parent stars. Baraffe et al. (2005) showed that the hot-Neptune planets could originate from more massive gas giants that have experienced significant evaporation. Thus, a further study on the evolution of the residual core is expected.

Currently, hydrodynamic models favor intermediate mass loss rates (Yelle 2004; Tian et al. 2005; Murray-Clay et al. 2009). However, the accurate X-ray transfer model of Cecchi-Pestellini et al. (2006) showed that the heating rates are significantly higher than those calculated by Yelle (2004), and the X-ray irradiation could be still significant for the planets even at a large separation. Moreover, we also neglect the inflation of radius due to tidal heating, which could induce a stronger hydrodynamic process on the upper atmosphere of planet. Consequently, an accurate model with mass loss, tidal heating, and tidal migration is expected.

The equations of tidal evolution are not accurate because the effect of the spin of the star is omitted in them. However, the basic conclusion should be the same even if the rotation of the star is taken into account because the young star rapidly loses angular momentum on account of magnetized wind. The properties of host star are fixed in our integrations. In fact, the life of a main-sequence dwarf star is about 10 Gyr. For long-life planets, the evolutions of their host stars should be considered.

In this paper, we investigated the tidal evolution and the mass loss of close-in extrasolar planets and research how both of them affect the evolutions of orbit and mass. For close-in planets, the mass loss can produce an important influence on the tidal evolution. Our models show that the effect of mass loss depends not only on the mass, the separation, and the eccentricity, but also on the radius $R1$ at the distance of which the bulk of XUV radiation is absorbed. With the assumption of $\beta = 3$, the effect of mass loss is remarkable on the planets with low mass at $a \leqslant 0.1$ AU. With the assumption of $\beta = 1.1$, the loss process could only affect the planets with low mass at $a \sim 0.05$ AU. Under both circumstances, the effect of mass loss on massive planets can be neglected.

We also discussed the influence of heating efficiency on tidal evolution. Our results show that mass loss is still useful for tidal evolution when heating efficiency is as low as 25%. Our models can be applied to the evolution models and planet population synthesis models. For example, the population synthesis models with tidal migration could be helpful to explain the distribution of planet. As the mass loss is considered into the evolution of single planet, the properties of planet can be determined. The properties of HD 209458b can be explained by our model.

I am grateful to the referee for a constructive suggestion that led to substantive improvements in this work. This work was supported by the National Natural Science Foundation of China (No. 10803018), the Knowledge Innovation Program of Chinese Academy of Sciences (07ACX21001), and the Western Light Talent Culture Project of The Chinese Academy of Sciences (08AXB31001).

REFERENCES

Adams, E. R., Seager, S., & Elkins-Tanton, L. 2008, ApJ, 673, 1160
Arras, P., & Bildsten, L. 2006, ApJ, 650, 394
Baraffe, I., Chabrier, G., Barman, T. S., Selsis, F., Allard, F., & Hauschildt, P. H. 2005, A&A, 436, L47
Baraffe, I., Selsis, F., Chabrier, G., Barman, T. S., Allard, F., Hauschildt, P. H., & Lammer, H. 2004, A&A, 419, L13
Barnes, R., Raymond, S. N., Jackson, B., & Greenberg, R. 2008, Astrobiology, 8, 557
Bodenheimer, P., Lin, D. N. C., & Mardling, R. A. 2001, ApJ, 548, 466
Burrows, A., Hubeny, I., Budaj, J., & Hubbard, W. B. 2007, ApJ, 661, 502
Cecchi-Pestellini, C., Ciaravella, A., & Micela, G. 2006, A&A, 458, L13
Dobbs-Dixon, I., Lin, D. N. C., & Mardling, R. A. 2004, ApJ, 610, 464
Donati, J. F., et al. 2008, MNRAS, 385, 1179
Eggleton, P. P., & Kiseleva, L. G. 1998, ApJ, 499, 853
Erkaev, N. V., Kulikov, Y. N., Lammer, H., Selsis, F., Langmayr, D., Jaritz, G. F., & Biernat, H. K. 2007, A&A, 472, 329
Fortney, J. J., Marley, M. S., & Barnes, J. W. 2007, ApJ, 659, 1661
Gu, P. G., Bodenheimer, P. H., & Lin, D. N. C. 2004, ApJ, 608, 1076
Guillot, T., & Showman, A. P. 2002, A&A, 385, 156
Hansen, B. M. S., & Barman, T. 2007, ApJ, 671, 861
Hellier, C., et al. 2009, Nature, 460, 1098
Hut, P. 1980, A&A, 92, 167
Ibgui, L., & Burrows, A. 2009, ApJ, 700, 1921
Jackson, B., Barnes, R., & Greenberg, R. 2009, ApJ, 698, 1357
Jackson, B., Greenberg, R., & Barnes, R. 2008, ApJ, 678, 1396
Lammer, H., Selsis, F., Ribas, I., Guinan, E. F., Bauer, S. J., & Weiss, W. W. 2003, ApJ, 598, L121
Lammer, H., et al. 2009, A&A, 506, 399
Lecavelier des Etangs, A. 2007, A&A, 461, 1185
Lecavelier des Etangs, A., Vidal-Madjar, A., McConnell, J. C., & Hébrard, G. 2004, A&A, 418, L1
Mazeh, T., Zucker, S., & Pont, F. 2005, MNRAS, 356, 955
Melo, C., Santos, N. C., Pont, F., Guillot, T., Israelian, G., Mayor, M., Queloz, D., & Udry, S. 2006, A&A, 460, 251
Miller, N., Fortney, J. J., & Jackson, B. 2009, ApJ, 702, 1413
Murray-Clay, R. A., Chiang, E. I., & Murray, N. 2009, ApJ, 693, 23
Penz, T., Micela, G., & Lammer, H. 2008, A&A, 477, 309
Pont, F. 2009, MNRAS, 396, 1789
Rasio, F. A., Tout, C. A., Lubow, S. H., & Livio, M. 1996, ApJ, 470, 1187
Seager, S., Kuchner, M., Hier-Majumder, C. A., & Militzer, B. 2007, ApJ, 669, 1279
Skumanich, A. 1972, ApJ, 171, 565
Southworth, J., Wheatley, P. J., & Sams, G. 2007, MNRAS, 379, 11
Tian, F., Toon, O. B., Pavlov, A. A., & De Sterck, H. 2005, ApJ, 621, 1049
Vidal-Madjar, A., Lecavelier des Etangs, A., Désert, J.-M., Ballester, G. E., Ferlet, R., Hébrard, G., & Mayor, M. 2003, Nature, 422, 143
Watson, A. J., Donahue, T. M., & Walker, J. C. G. 1981, Icarus, 48, 150
Yelle, R. 2004, Icarus, 170, 167
Zahn, J. P. 1977, A&A, 57, 383